

CASE REPORT OPEN ACCESS

# Real-Time Subcutaneous Arterial Navigation for Thinning of an Anterolateral Thigh Flap Using Photoacoustic Imaging and Projection Mapping: A Case Report

Itaru Tsuge<sup>1</sup>  | Susumu Saito<sup>1</sup> | Maria Chiara Munisso<sup>1</sup> | Tomoko Kosaka<sup>1</sup> | Ayako Takaya<sup>1</sup> | Chang Liu<sup>2</sup> | Goshiro Yamamoto<sup>2</sup> | Naoki Morimoto<sup>1</sup>

<sup>1</sup>Department of Plastic and Reconstructive Surgery, Graduate School of Medicine, Kyoto University, Kyoto, Japan | <sup>2</sup>Department of Medical Informatics, Graduate School of Medicine, Kyoto University, Kyoto, Japan

**Correspondence:** Itaru Tsuge ([itsuge@kuhp.kyoto-u.ac.jp](mailto:itsuge@kuhp.kyoto-u.ac.jp))

**Received:** 16 March 2024 | **Revised:** 15 October 2024 | **Accepted:** 26 December 2024

**Funding:** This research was supported by the Japan Agency for Medical Research and Development (AMED) under grant number JP19he2302002.

**Keywords:** anterolateral thigh | free flap | navigation | photoacoustic | projection mapping

## ABSTRACT

Thinning of anterolateral thigh flap is challenging. Anatomical studies have shown variations in arterial branching patterns in the subcutaneous layer, which were suspected to be the reason for the high frequency of thinning failures. We attempted to visualize subcutaneous arterial courses preoperatively and perform thinning of perforator flaps using this information appropriately. We accumulated evidence on the accuracy of noninvasive vascular visualization using photoacoustic tomography (PAT). In the present case, we applied a medical imaging projection system (MIPS), which enabled real-time surgical navigation using indocyanine green (ICG) emission signals, to use photoacoustic information intraoperatively during the flap thinning procedure. A 69-year-old woman underwent half-tongue resection using the pull-through method for right-sided tongue cancer. Preoperative PAT was performed 5 days before surgery. The 12×6-cm area took ~8 min to scan. We used an ICG test card containing ICG-positive control material cut into strips to show tentative artery lines by projection mapping. The transparent vascular map was laminated and sterilized. MIPS captured ICG fluorescence signals that penetrated the anterolateral thigh flap and continuously projected the purple area on the reverse side of the flap, guiding the position of the tentative arteries. A 20×6.5-cm anterolateral thigh flap was elevated with the distal part of the reconstructed tongue and proximal de-epithelialized part to fill the pull-through tunnel in the submandibular region. Active bleeding was observed when cutting marginal fat tissue near the purple line of the distal ALT flap projected by MIPS. The study protocol did not include a highly invasive trial for MIPS-guided thinning; therefore, we removed minimal marginal fat tissue. The ALT flap showed no postoperative complications while maintaining conversation and swallowing functions. We present the concept of subcutaneous arterial real-time navigation surgery using PAT and MIPS for safe, easy, and fast flap thinning procedures in the future.

## 1 | Introduction

Nearly 20 years ago, a thinning technique for the anterolateral thigh (ALT) flap was proposed (Kimura and Satoh 1996); however, follow-up clinical reports have highlighted the instability of flap blood circulation, resulting in necrosis (Ross et al. 2003;

Alkureishi, Shaw-Dunn, and Ross 2003). In 2008, anatomical studies revealed that ALT flap perforators had three types of subcutaneous arterial branching patterns, which seemed to cause a high frequency of thinning failures in types 2 and 3, including horizontal arterial connections within the suprafascial plexus (Schaverien et al. 2008). The microdissection procedure,

This is an open access article under the terms of the [Creative Commons Attribution-NonCommercial-NoDerivs](https://creativecommons.org/licenses/by-nc-nd/4.0/) License, which permits use and distribution in any medium, provided the original work is properly cited, the use is non-commercial and no modifications or adaptations are made.

© 2025 The Author(s). *Microsurgery* published by Wiley Periodicals LLC.

in which the subcutaneous vessels are microscopically dissected, is the only way to make the primary thinning procedure safer (Kimura, Satoh, and Hosaka 2003); however, its performance is not widespread because of its complexity and the risk of flap necrosis.

Preoperative imaging, which helps surgeons understand the comprehensive courses of subcutaneous arteries and veins, leads to the establishment of safe thinning surgery. We attempted to visualize the subcutaneous branching patterns of ALT perforators using photoacoustic tomography (PAT) and proved its accuracy in a clinical trial (Tsuge et al. 2018; Tsuge et al. 2020). In PAT, near-infrared pulsed laser light energy is absorbed by hemoglobin, which causes rapid thermo-elastic deformation allowing ultrasonic transducers to detect and generate images of blood vessels. The S-factor is an approximate value that correlates with hemoglobin oxygen saturation by switching pulse-to-pulse wavelengths of 756 and 797 nm (Matsumoto et al. 2018). The segment mode constructed from the S-factor value shows the tentative arteries and veins in red and blue, respectively.

We previously demonstrated that preoperatively selected tentative arteries matched with intraoperative indocyanine green (ICG) angiography (Tsuge, Munisso, et al. 2023; Munisso et al. 2024). Our purpose was to visualize subcutaneous arterial courses preoperatively and to perform thinning of perforator flaps using this information appropriately. In this case, we applied a medical imaging projection system (MIPS; Mitaka Kohki, Tokyo, Japan), which enabled real-time surgical navigation using ICG emission signals (Tsuge et al. 2021; Tsuge, Sowa, et al. 2023), to use photoacoustic information intraoperatively during the flap thinning procedure.

We herein report the first case of intraoperative real-time projection mapping navigation surgery visualizing the subcutaneous arteries from the reverse side of an elevated ALT flap using MIPS.

## 2 | Case Report

The patient was a 69-year-old woman with right tongue cancer noticed by experiencing pain for 3 months (Figure 1a). Twenty-two years earlier, she had undergone right partial tongue resection for tongue cancer (T1N0M0). She had no history of alcohol consumption or smoking. Half-tongue resection using pull-through surgery (Ferri et al. 2020) with bilateral cervical lymph node dissection was planned; therefore, we prepared reconstruction surgery using a free ALT flap.

A PAT imaging system (LUB-0) produced by Luxonus (Kanagawa, Japan) was used (Tsuge, Munisso, et al. 2023; Munisso et al. 2024). PAT was performed 5 days before the surgery. The 12×6-cm area took ~8 min to scan. The segment mode constructed from the S-factor showed separation of the tentative arteries and veins (Figure 1b). We applied the PreFlap protocol proposed in 2024 (Munisso et al. 2024), which contains a new algorithm for converting three-dimensional PAT images to two-dimensional vascular mapping sheets for perforator flap surgeries. Furthermore, to use MIPS in the surgical field, the ICG test card produced by Mitaka Kohki was cut into strips (Figure 1c)

and pasted on the tentative artery lines of the transparent vascular map, which was laminated and sterilized using a method in our previous report (Tsuge et al. 2020) (Figure 1d).

After covering the reference crosses marked at 2-cm intervals with sterilized film sheets (Figure 2a), a 20×6.5 cm ALT flap containing two perforators was elevated from the right thigh (Figure 2b,c). A skin incision around the flap reduced the area by ~10%. The ICG test card generated signals by itself; therefore, we attempted to capture the signals positioned beneath the flap and projected them onto it. We turned the transparent vascular map upside down and called it the reverse (Figure 2d). The ALT flap was also turned upside down and placed on a vascular map. To fit the shrunken flap to the reference points of the underlaid map, we used yellow sponges of the needle counter pasted on the map and sutured to the edge of the flap. MIPS detected ICG signals that penetrated the flap and projected the purple area continuously, guiding the position of the tentative subcutaneous arteries (Figure 3a). Interestingly, active bleeding was observed when the marginal fat tissue was cut near the projected purple line (Video S1). Finally, to confirm the accuracy of the PAT vascular maps, intraoperative ICG angiography by intravenous injection to compare their matches was performed using our previously reported method (Tsuge, Munisso, et al. 2023). Both the early and late phases matched the tentative arterial and venous maps, respectively (Figure 3b,c).

The proximal part of the ALT flap was deepithelialized to fill the submandibular tunnel (Figure 4a). The descending branch of the lateral femoral circumflex artery and the two veins were microscopically anastomosed to the right superior thyroid artery, right common facial vein, and right external jugular vein (Figure 4b,c). The ischemic time of the ALT flap was 83 min. The total operative time was 10 h and 9 min. Postoperatively, no complications such as blood circulation disorder, wound dissection, fistula, or infection were observed. The tumor resection margin was negative (T3N2bM0). She was able to eat and speak without any problems 4 months postoperatively (Figure 4d).

## 3 | Discussion

We applied MIPS to use PAT information intraoperatively during the flap thinning procedure. This is the first case of intraoperative real-time projection mapping navigation surgery that visualized the subcutaneous arteries from the reverse side of the elevated ALT flap.

The microdissection procedure (Kimura, Satoh, and Hosaka 2003) is the only way to make the primary thinning procedure safer. Kimura et al. (2006) introduced the technique of dissecting the adipose layer microscopically and removing large fat lobules of the deep adipose layer from around the perforators, which usually produces several branches before reaching the superficial adipose layer. However, the procedure has not become widespread owing to its complexity and the risk of flap necrosis (Ross et al. 2003; Alkureishi, Shaw-Dunn, and Ross 2003). Anatomical studies have revealed that ALT flap perforators have three types of subcutaneous arterial branching patterns, which seem to cause a high frequency of thinning failure in types 2 and 3, including

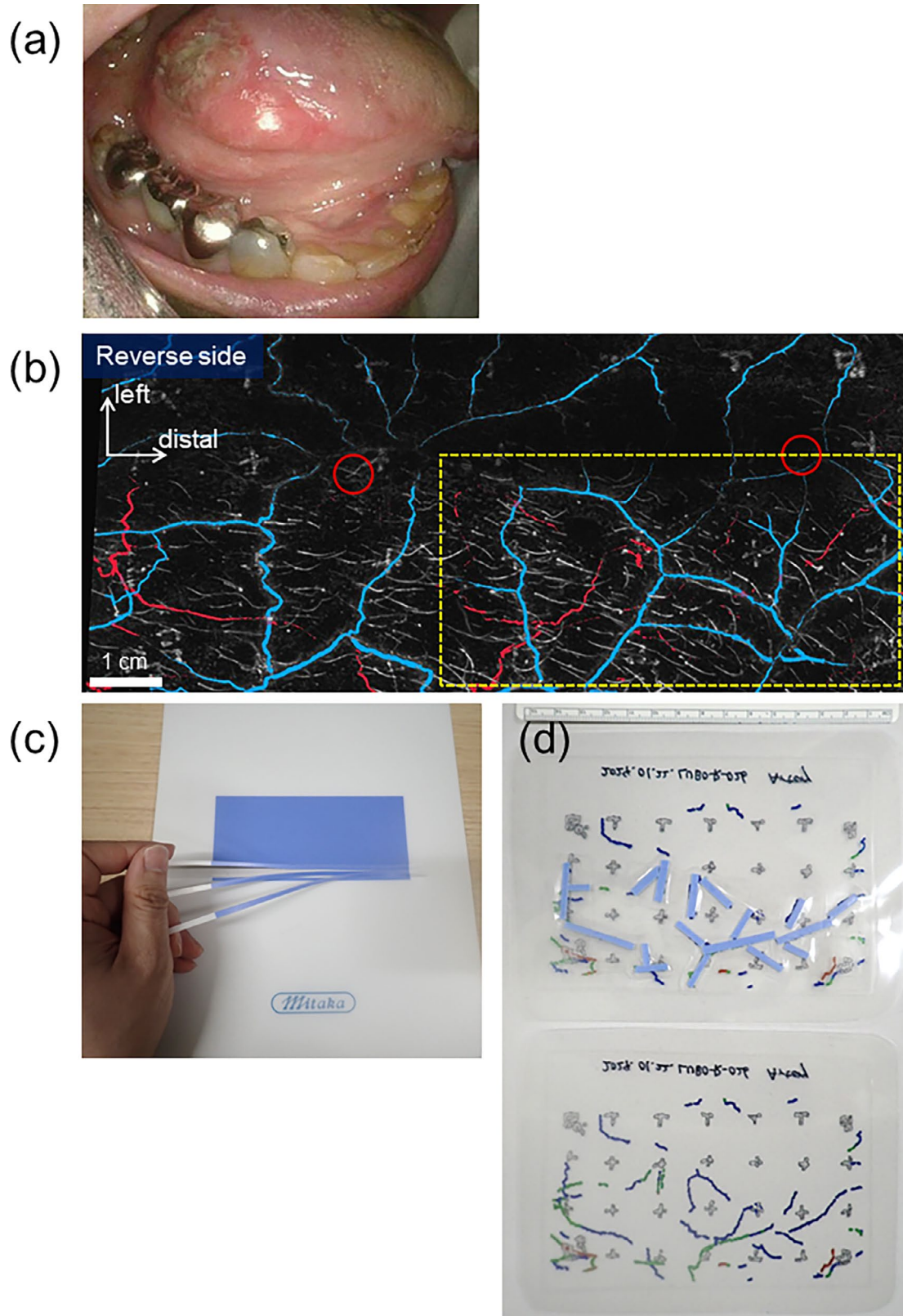


**FIGURE 1** | (a) Preoperative finding of right tongue cancer. (b) Photoacoustic imaging of the 12×6 cm area in the right anterolateral thigh. The segment mode constructed from the S-factor value shows the tentative arteries and veins as red and blue, respectively. Red circles are the fasciapenetrating points of perforators detected by ultrasonography. The dotted rectangular area indicates the same area as shown in Figures 2 and 3. (c) ICG test card strips generate signals by themselves. (d) ICG test card strips are laminated to show the tentative artery lines.

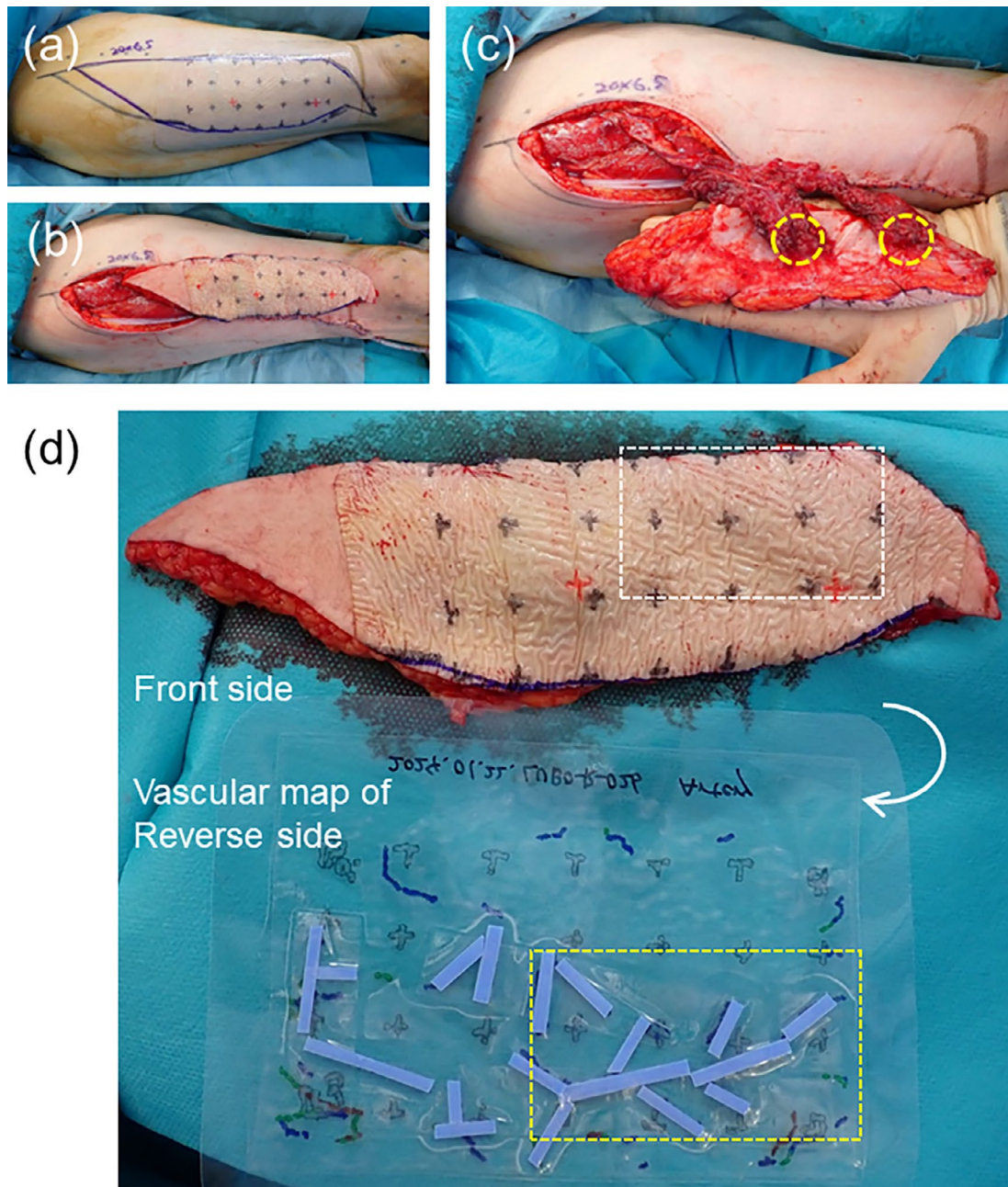


**FIGURE 2** | (a) The reference crosses preserved by sterilized film are set at 2-cm intervals. (b) The size of a right ALT flap is 20×6.5 cm. (c) Two perforators are indicated by yellow-dotted circles. (d) The ALT flap is still vascularized under the blue sheets. The sterilized transparent vascular map is turned upside down; therefore, the white-dotted square in the flap is the same area as the yellow-dotted square in the map.

horizontal arterial connections within the suprafascial plexus (Schaverien et al. 2008). However, PAT has an excellent ability to visualize blood vessels in the horizontal direction, making it ideal for the vascular network analysis of subcutaneous perforators (Tsuge et al. 2018; Tsuge et al. 2020).

Pull-through surgery for tongue resection with en bloc neck nodes without mandible splitting is a recent common technique for otorhinolaryngologists, usually being followed by free flap reconstruction because of the subsequent large surgical defect (Ferri et al. 2020). Therefore, the proximal part of the ALT flap was de-epithelialized as the volume for filling the pull-through tunnel to prevent leaks and fistulas. However, the reconstructed

tongue should be a thin and flexible flap, which requires a complex design for high-quality reconstruction.

To make the thinning procedure safer, we need to not only create detailed maps but also enable the information to be easily referred to intraoperatively. If we apply the sheet-type vascular map, we cannot check the reference markings on the front side of the flap when performing thinning on the reverse side. We created an arterial map including the ICG test card strips, which generated signals by themselves, to detect them positioned beneath the flap and project them onto the reverse side of the elevated ALT flap. We did not evaluate this detection using a near-infrared light microscope camera to visualize ICG

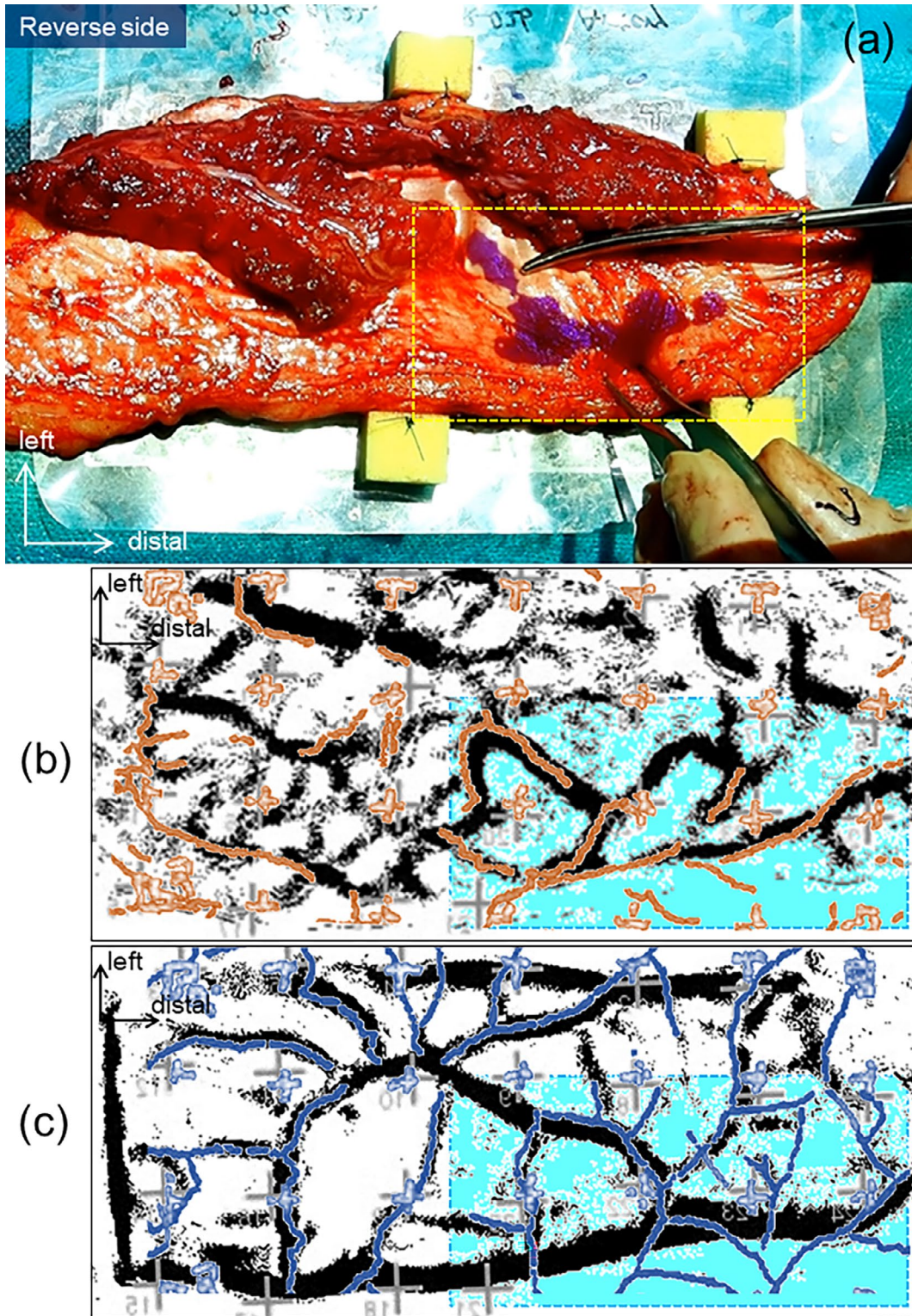


**FIGURE 3** | (a) Real-time MIPS navigation for thinning of the flap. The purple area is the projected image from the MIPS. The ICG signal of the test card strips penetrates the ALT flap, navigating the position of subcutaneous arterial courses. (b) A merged image of tentative arteries PAT vascular map (orange lines) and ICG angiography image in the early arterial phase (black lines). The blue square is the same area as the dotted squares in Figure 4a. (c) A merged image of tentative veins on the PAT vascular map (blue lines) and an ICG angiography image in the late venous phase (black lines).

signals. The study protocol did not include a highly invasive trial for MIPS-guided thinning; therefore, we removed only a small amount of marginal fat in this case. We can thus only present

the concept of subcutaneous arterial real-time navigation surgeries using PAT and MIPS for safe, easy, and fast flap thinning procedures in the future.

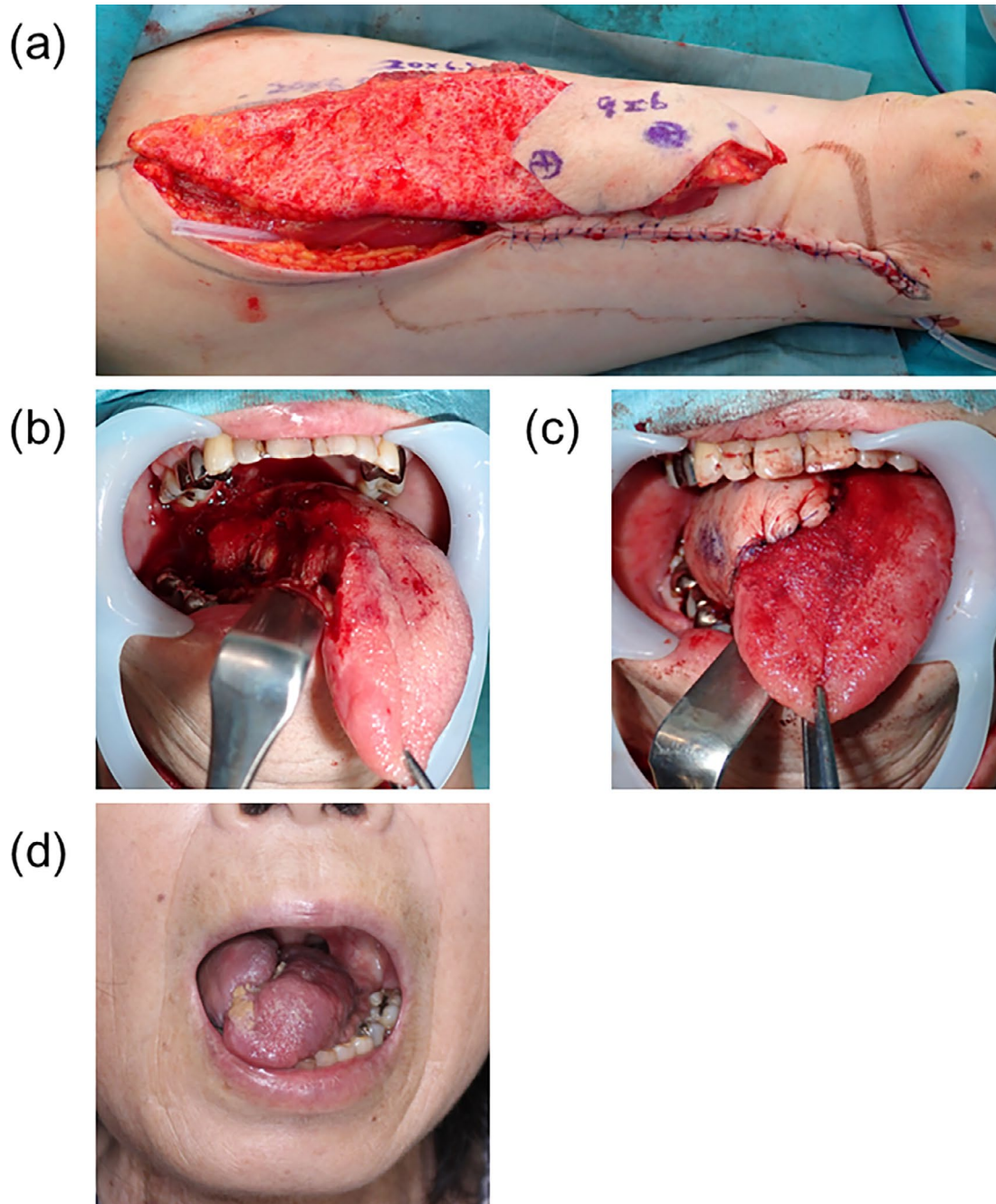


**FIGURE 4** | (a) The proximal part is de-epithelialized as volume for filling the submandibular tunnel. (b) The right half of the tongue is resected. (c) The distal 9×6-cm part of the ALT flap is sutured to cover the defect. (d) Postoperative findings of the tongue at 4 months.

Further studies and improvements are required to increase the accuracy and simplicity. However, we believe that PAT and MIPS have the potential facilitate real-time navigation in flap surgery.

#### Acknowledgments

This research was supported by the Japan Agency for Medical Research and Development (AMED) under grant number JP19he2302002. The authors used a photoacoustic imaging system made by Luxonus Inc., Kanagawa, Japan.

#### Ethics Statement

This study was approved by the ethics committee of the Kyoto University Graduate School of Medicine (Y0083) and conducted in accordance with the Declaration of Helsinki.

#### Consent

Written informed consent was obtained from the patient.

#### Conflicts of Interest

The authors declare no conflicts of interest.

## Data Availability Statement

The data that support the findings of this study are available from the corresponding author upon reasonable request.

## References

- Alkureishi, L. W., J. Shaw-Dunn, and G. L. Ross. 2003. "Effects of Thinning the Anterolateral Thigh Flap on the Blood Supply to the Skin." *British Journal of Plastic Surgery* 56: 401–408.
- Ferri, A., G. Perlangeli, N. Montalto, et al. 2020. "Transoral Resection With Buccinator Flap Reconstruction vs. Pull-Through Resection and Free Flap Reconstruction for the Management of T1/T2 Cancer of the Tongue and Floor of the Mouth." *Journal of Cranio-Maxillo-Facial Surgery* 48: 514–520.
- Kimura, N., M. Saito, Y. Itoh, and N. Sumiya. 2006. "Giant Combined Microdissected Thin Thigh Perforator Flap." *Journal of Plastic, Reconstructive & Aesthetic Surgery* 59: 1325–1329.
- Kimura, N., and K. Satoh. 1996. "Consideration of a Thin Flap as an Entity and Clinical Applications of the Thin Anterolateral Thigh Flap." *Plastic and Reconstructive Surgery* 97: 985–992.
- Kimura, N., K. Satoh, and Y. Hosaka. 2003. "Microdissected Thin Perforator Flaps: 46 Cases." *Plastic and Reconstructive Surgery* 112: 1875–1885.
- Matsumoto, Y., Y. Asao, H. Sekiguchi, et al. 2018. "Visualizing Peripheral Arterioles and Venules Through High-Resolution and Large-Area Photoacoustic Imaging." *Scientific Reports* 8: 14930.
- Munisso, M. C., C. Liu, G. Yamamoto, et al. 2024. "PreFlap: From Photoacoustic Tomography Images to Vascular Mapping Sheets for Improved Preoperative Flap Evaluation." *IEEE Transactions on Biomedical Engineering* 71: 139–149.
- Ross, G. L., R. Dunn, J. Kirkpatrick, et al. 2003. "To Thin or Not to Thin: The Use of the Anterolateral Thigh Flap in the Reconstruction of Intraoral Defects." *British Journal of Plastic Surgery* 56: 409–413.
- Schaverien, M., M. Saint-Cyr, G. Arbique, D. Hafez, S. A. Brown, and R. J. Rohrich. 2008. "Three- and Four-Dimensional Computed Tomographic Angiography and Venography of the Anterolateral Thigh Perforator Flap." *Plastic and Reconstructive Surgery* 121: 1685–1696.
- Tsuge, I., M. C. Munisso, T. Kosaka, et al. 2023. "Preoperative Visualization of Midline-Crossing Subcutaneous Arteries in Transverse Abdominal Flaps Using Photoacoustic Tomography." *Journal of Plastic, Reconstructive & Aesthetic Surgery* 84: 165–175.
- Tsuge, I., S. Saito, H. Sekiguchi, et al. 2018. "Photoacoustic Tomography Shows the Branching Pattern of Anterolateral Thigh Perforators In Vivo." *Plastic and Reconstructive Surgery* 141: 1288–1292.
- Tsuge, I., S. Saito, G. Yamamoto, et al. 2020. "Preoperative Vascular Mapping for Anterolateral Thigh Flap Surgeries: A Clinical Trial of Photo Acoustic Tomography Imaging." *Microsurgery* 40: 324–330.
- Tsuge, I., Y. Sowa, H. Yamanaka, M. Katsube, M. Sakamoto, and N. Morimoto. 2023. "Real-Time Navigation for Vascularized Lymph-Node Transplantation Using Projection Mapping With Indocyanine Green Fluorescence." *Plastic and Reconstructive Surgery. Global Open* 11: e4743.
- Tsuge, I., H. Yamanaka, S. Seo, et al. 2021. "A Novel Real-Time Navigation System for Lymphaticovenular Anastomosis Using Projection Mapping With Indocyanine Green Fluorescence." *Plastic and Reconstructive Surgery. Global Open* 9: e3758.

## Supporting Information

Additional supporting information can be found online in the Supporting Information section.